Torque Scaling Laws for Interior and Exterior Rotor Permanent Magnet Machines

Thomas Reichert[1], Thomas Nussbaumer[2], Johann W. Kolar[1]

[1]Power Electronic Systems Laboratory, ETH Zurich, 8092 Zurich, Switzerland
[2]Levitronix GmbH, Technoparkstrasse 1, 8005 Zurich, Switzerland

The paper provides a general comparison of permanent magnet machines of interior and exterior rotor type based on scaling laws. The main goal is to maximize the torque for given machine dimensions. Particularly, analytical equations are derived which allow a general evaluation of the two construction types for their suitability in dependency on rotor and stator dimensions. Using 3D-FEM simulations, the equations are verified and saturation effects are taken into account.

***Index Terms*—scaling laws, external rotor, internal rotor, high-torque, permanent magnet motors**

I. Introduction

In a wide range of applications, such as pumps, mixers, stirrers, etc., high torque is required for permanent magnet (PM) machines for given machine dimensions. Basically, two motor construction types exist, namely the interior rotor type (cf. Fig. 1) and the exterior rotor type (cf. Fig. 2).

The interior rotor configuration allows a very compact setup, since the rotor can be built very small. However, this results in a small torque due to the short lever arm being the air gap radius. If the air gap radius is enlarged, the rotor is usually constructed as a hollow rotor ring (cf. Fig. 1), which results in the loss of valuable motor space in the center. Additionally, for given outer dimensions of the motor, the space for the stator carrying the motor coils (and therefore, the producible motor torque) is reduced for a larger air gap. Thus, the maximum torque can be found by optimization, which will be derived in this paper.

For the exterior rotor configuration, on the other hand, all the windings have to be placed in the inner part of the motor (cf. Fig. 2), so the space for the stator with the coils is limited. This means that the air gap radius has to be larger than a certain minimum value so that the exterior rotor configuration makes sense in terms of torque compared to the interior rotor type. In literature, many performance optimizations have been done yet for either interior [1]-[3] or exterior rotor machines [4]-[7]. In [8], both machine types have been compared for the special case of auxiliary salient poles. However, no detailed general comparison of these two machine concepts has been undertaken so far.

Hence, in this paper, a comparative evaluation of the two radial-flux machine configurations will be performed based on general scaling laws and meaningful assumptions. This allows the reader to evaluate the concepts for any given motor specification and select the appropriate motor configuration.

The taken assumptions are explained in section II. In section III, the producible torque is calculated for both machine types and the two types are compared analytically. In chapter IV, the equations are verified using 3D-FEM simulations and the influence of real limitations (magnetic saturation) is analyzed and discussed.

Digital Object Identifier inserted by IEEE

II. Assumptions

For the analytical comparison of the two configurations, the following assumptions have been made:

- The comparison is undertaken for fixed outer machine dimensions; therefore, the outer machine radius R and the machine length l are determined. The influencing variable is the air gap radius r, which divides the available space between the rotor and the stator.
- It is assumed that the air gap (with radial thickness δ) is chosen very narrow. Therefore, magnetic leakage can be

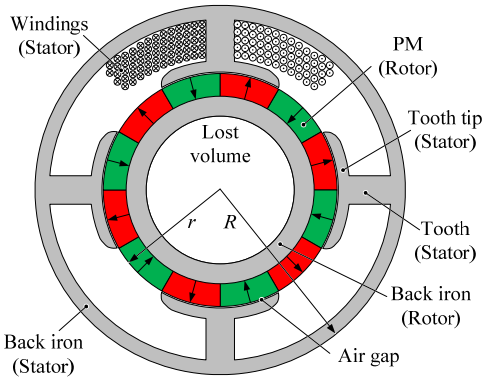

Fig. 1. Interior rotor machine with air gap radius r and outer radius R.

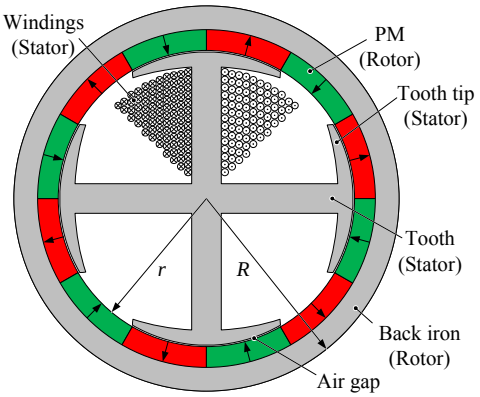

Fig. 2. Exterior rotor machine with air gap radius r and outer radius R.

neglected and the discussion can be reduced to a two-dimensional problem.

- The magnetic flux density B due to the permanent magnets in the air gap is assumed to be constant for all possible configurations with different air gap radius r. This assumption is legitimate for very small air gap thickness δ, when the radial thickness of the permanent magnets δ_{PM} becomes dominant ($\delta_{PM} >> \delta$). According to the formula

$$B \approx B_r \cdot \left(\frac{\delta_{PM}}{\delta_{PM} + \delta} \right), \quad (1)$$

the air gap magnetic flux density B is then close to the magnet's remanence B_r. This assumption is verified and discussed later especially under consideration of non-ideal conditions with magnetic saturation.

- A certain percentage c_w of the stator area is used for the stator windings, while the remaining area is needed for either iron or mechanical fixations (e.g. Hall sensors for position detection). It is assumed that the percentage for the winding area is constant for both interior and exterior rotor setup and independent of the air gap radius r

$$A_{wdg} = c_w \cdot A_{stator} . \quad (2)$$

This assumption is also critical in terms of magnetic saturation and will be further discussed later in this paper.

- The maximum allowed current density in the stator windings is constant for all configurations. The product of the number of winding turns N and the current I is the magnetomotive force θ measured in ampere-turns. It is limited by the maximum current density J_{max} multiplied with the winding area

$$\theta_{max} = (N \cdot I)_{max} = J_{max} \cdot A_{wdg} . \quad (3)$$

The maximum allowed current density mainly depends on the type of cooling system implemented with the machine. In the following, the torque is calculated for a certain given maximum current density value.

III. Torque Calculation and Comparison

The torque calculation in a radial-flux machine is based on the (tangential) Lorentz force

$$F = B \cdot (N \cdot I)_{max} \cdot l = B \cdot J_{max} \cdot A_{wdg} \cdot l \quad (4)$$

with B being the magnetic air gap flux density and l the length of the machine. According to the assumptions previously made, the only non-constant factor in (4) is the area for the stator windings A_{wdg}. Combining (4) and (2) reveals the linear relation between Lorentz force and stator area

$$F = B \cdot J_{max} \cdot l \cdot c_w \cdot A_{stator} = c_F \cdot A_{stator} \quad (5)$$

with a force constant c_F.

The torque of the machine is then given by multiplying the Lorentz force on the rotor with the air gap radius

$$T = F \cdot r \sim A_{stator} \cdot r . \quad (6)$$

A. Ideal torque of interior rotor machine

For the interior rotor machine, the surface area of the stator depends on the total machine radius R and the air gap radius r

$$F \sim A_{stator} = (R^2 - r^2) \cdot \pi . \quad (7)$$

The resulting torque becomes a function of R and r

$$T \sim (R^2 - r^2) \cdot r = (1 - x_r^2) \cdot x_r \cdot R^3 , \quad (8)$$

where $x_r = r/R$, thus the ratio of the air gap radius r to the outer machine radius R. Moreover, (8) reveals the scaling factor R^3 which is also found in [9]. This means that the torque would grow with a cubic factor if the total machine area was enlarged. We can complete (8) to

$$\frac{T}{c_F \cdot \pi \cdot R^3} = \left(1 - \frac{r^2}{R^2} \right) \cdot \frac{r}{R} = (1 - x_r^2) \cdot x_r . \quad (9)$$

Furthermore, the torque can be calculated as a function of $x_A = A_{stator} / A_{motor}$, thus the ratio of stator area to motor area. For the interior rotor machine, this ratio becomes

$$x_A = \frac{\pi \cdot (R^2 - r^2)}{\pi \cdot R^2} = 1 - x_r^2 . \quad (10)$$

Solving (10) for x_r and substituting x_r in (9) yields

$$\frac{T}{c_F \cdot \pi \cdot R^3} = x_A \cdot \sqrt{1 - x_A} . \quad (11)$$

B. Ideal torque of exterior rotor machine

For the exterior rotor machine, the surface area of the stator only depends on the air gap radius r

$$F \sim A_{stator} = r^2 \cdot \pi . \quad (12)$$

In this case, the resulting torque becomes

$$T \sim r^3 = x_r^3 \cdot R^3 . \quad (13)$$

For the exterior rotor, it is obvious that the torque grows with the air gap radius r for fixed machine radius R. There is an upper limit for r which depends on R, since a certain minimum space for the rotor magnets is needed. In (13) it can be seen that the torque for the exterior rotor machine also grows with the factor R^3. Equation (13) can be completed to

$$\frac{T}{c_F \cdot \pi \cdot R^3} = \frac{r^3}{R^3} = x_r^3 . \quad (14)$$

Once more, the torque is also calculated as a function of stator area to total motor area. This time, this ratio becomes

$$x_A = \frac{\pi \cdot r^2}{\pi \cdot R^2} = x_r^2 . \quad (15)$$

Combining (14) and (15) leads to

$$\frac{T}{c_F \cdot \pi \cdot R^3} = \sqrt{x_A^3} . \quad (16)$$

C. Analytical torque comparison

For the comparison of the torque capabilities, the producible torque for changing air gap radius is plotted in Fig. 3(a). It can be seen that for a small ratio of air gap radius to machine radius, the interior motor is advantageous, whereas the highest torque can theoretically be achieved with the exterior rotor type for the largest possible air gap radius $r = R$ ($x_r = 1$). In reality, the achievable maximum value for x_r depends on the radial thickness of the magnets δ_{PM} and of the rotor back iron.

In Fig. 3(a) the comparison between interior and exterior

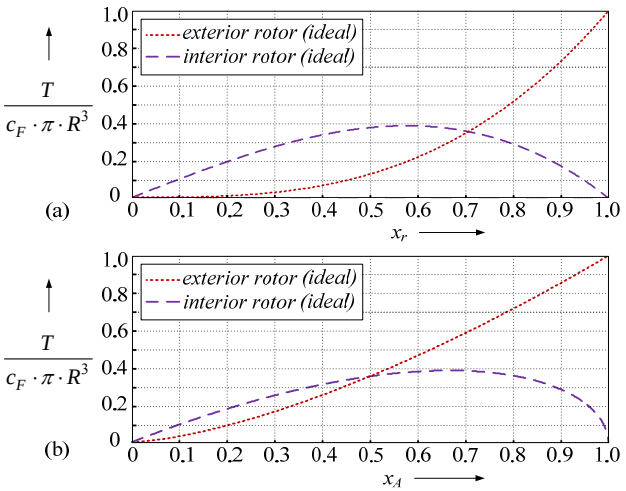

Fig. 3. Producible torque for both topologies as a function of (a) ratio $x_r = r/R$ and (b) $x_A = A_{stator}/A_{motor}$

rotor is not yet obvious, since in the first case (interior rotor) it is the rotor that grows with the air gap radius, whereas in the second case (exterior rotor) it is the stator. Therefore, the comparison is also made as a function of stator area to machine area and depicted in Fig. 3(b).

The intersection of the torque for the interior rotor and exterior rotor machine is exactly in case of equal areal space for both stator and rotor (resulting in an air gap radius of $r = R/\sqrt{2} \approx 0.707 \cdot R$). The interior rotor machine itself creates the highest possible torque, when the stator area is twice the rotor area (resulting in an air gap radius of $r = R/\sqrt{3} \approx 0.577 \cdot R$). However, at this optimum interior rotor point in Fig. 3(b), the exterior rotor machine is already advantageous. The exterior rotor machine becomes absolutely advantageous over the interior rotor machine when the ratio of stator area to the whole motor area exceeds 53% $\left(x_A \geq \sqrt[3]{4}/3 \approx 52.91\%\right)$. For a ratio higher than 84% $\left(x_A \geq \sqrt[3]{16}/3 \approx 84\%\right)$, the torque produced by the exterior rotor machine is theoretically already twice as big as the maximum possible torque of the interior rotor machine.

D. Realistic torque of interior rotor machine

In case of the interior rotor machine, the rotor back iron is located at the inside of the permanent magnet ring. Therefore, the radial thickness of the rotor back iron depends on the air gap radius r.

The rotor back iron would magnetically saturate for a small value of r, since this design would result in a large stator area allowing a very high number of ampere-turns (this problem could be avoided by omitting the rotor back iron and completely filling the rotor with permanent magnet material). If r is enlarged towards the optimal design point with $r = R/\sqrt{3}$, the number of ampere-turns is decreased and at the same moment the rotor back iron is enlarged. Therefore, magnetic saturation in the rotor back iron gets more and more unlikely. In practice, hollow rotor rings are built, since the radial thickness of the back iron can be reduced as long as no saturation occurs. The hollow rotor ring lowers the rotor's inertia, which is advantageous for transient applications, but as mentioned before, the motor space in the center is lost.

The magnetic saturation is essentially influenced by the design of the stator. As we will see in the next section, it is the winding space factor c_w that has to be optimized for the machine to provide maximum torque. In contrary to the exterior rotor type, the stator teeth of the interior rotor machine have to be connected with a back iron ring. Therefore, the available space for stator iron has to be divided between this back iron ring and the stator teeth.

E. Realistic torque of exterior rotor machine

Ideally, the torque of the exterior rotor grows extensively for a large air gap radius r (with a value close to the outer machine radius R). In reality however, two effects cause magnetic saturation in both rotor and stator iron, which in the end results in a lower air gap field B. First of all, the narrow rotor limits the radial thickness of the back iron ring for values of x_r close to 1. Therefore, the whole magnetic flux has to pass a very small area which is the product of back iron thickness and machine length. If this area gets too small, saturation will occur, which in consequence may lower the effective torque.

The second effect also depends on the air gap radius r. For growing r, the stator area gets enlarged, so that the magnetomotive force (in ampere-turns) grows with r^2. This force drives a magnetic flux through the stator and rotor iron which is superposed to the flux of the permanent magnets and the saturation problem is accelerated. Even though a higher number of ampere-turns is desired according to (4), it can even result in a decreasing torque when saturation effects heavily lower the air gap field. Moreover, this second effect depends on the factor c_w (winding area per stator area). If this factor is chosen large, the winding space is enlarged and therefore the number of ampere-turns. At the same time, the space for stator iron is reduced, so that there is less iron to drive the magnetic flux, which again results in saturation. As will be seen later, an optimum factor c_w and r can be found so that there is a good relation between high current and sufficient air gap field.

IV. Verification with 3D-FEM

Both setups with interior and exterior rotor have been simulated using Maxwell 3D [10]. An exemplary motor setup with four stator teeth and a pole pair number of six has been implemented. The simulation parameters are listed in Table I. The magnet material is NdFeB with a remanence flux density of 1.2 T. For the iron, two different materials have been chosen. Once, the setups have been simulated with the iron material M270-35A which shows saturation for high magnetic field. As a comparison, the same simulations have been repeated with an "ideal" iron material. This material's relative permeability is set to a constant value of $\mu_r = 6000$, and it is assumed that it never saturates ($B_{sat} \to \infty$). The stator teeth have been designed as square bars, and their widths w_t scale equally for both setups. This guarantees that the stator teeth enclose the same air gap width with the magnets for both interior and exterior rotor design. The geometric configuration of the stator of the exterior rotor machine defines the relation between the tooth width w_t, the air gap radius r and the

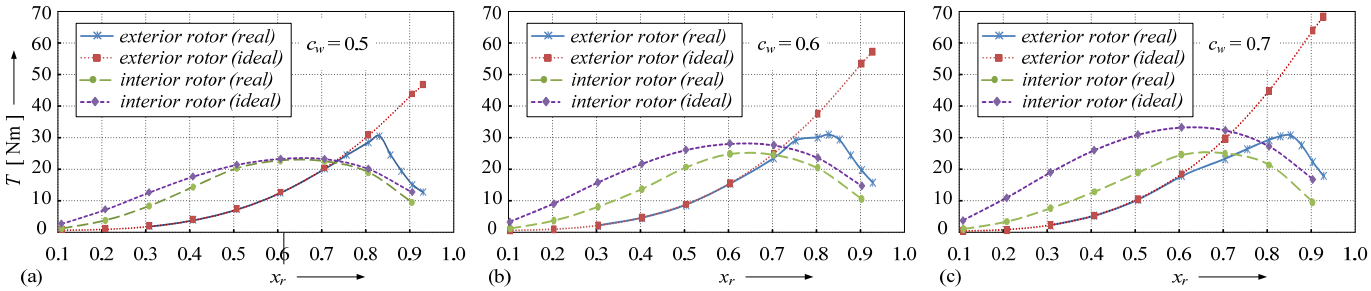

Fig. 4. Torque simulation for both motor setups with ideal and realistic constraints for values of c_w = 0.5 (a), 0.6 (b), and 0.7 (c).

winding space factor c_w. For this exemplary setup, this relation is $w_t = \sqrt{2}\cdot\left(1-\sqrt{c_w}\right)\cdot r$. In order to provide the same tooth width also for the interior rotor machine (and consequently similar magnetic conditions in the iron), the radial thickness of the stator back iron ring can be adapted such that the same value of c_w for both setups is achieved.

Fig. 4 shows simulation points for both setups and three different winding space factors c_w. It can be seen that under negligence of saturation effects the torque of the interior rotor depends on the air gap radius r as predicted by the analytical equations. For a small factor x_r and/or a large factor c_w, magnetic saturation occurs, which consequently limits the torque in reality. In the case of the exterior rotor machine, the simulations with "ideal" iron also confirm the predictions through analytical equations. In reality however, the torque is limited by the factor c_w and the air gap radius r, if it approaches the outer machine radius R, through saturation effects as discussed before. Therefore, an optimal design point can be found.

The simulations also proof our assumption of an equal factor c_w for both interior and exterior rotor. For the simulated design with equal tooth width w_t, the optimal factor is approximately the same for both setups ($c_w \approx 0.6$).

V. Conclusions

The analytical equations accurately predict the torque as long as no magnetic saturation occurs. It has been shown that for the interior rotor machine, the maximum torque can be found for a stator area to rotor area ratio of 2:1. The exterior rotor machine however requires the stator area to be as large as possible, just leaving enough space for the rotor to produce the required magnetic field. In this configuration, the exterior rotor machine could theoretically produce a much higher torque than achievable with the optimal interior rotor setup.

For real conditions however, the torque is reduced due to the lowered air gap field in case of magnetic saturation. Thus, the main design task consists in finding the optimum between a high number of ampere-turns and a high air gap field. The presented analytical equations and the simulations reveal that the exterior rotor design is the one with the higher possible torque. However, these equations do not predict the optimal design of such an exterior rotor. Many aspects, such as pole pair number, number of stator teeth, shape of stator, current density and, as shown in this paper, the factors c_w (winding space factor) and x_r (ratio of air gap radius to motor radius) influence the resulting torque.

The findings in this paper allow the reader to quickly evaluate the two topologies in terms of achievable torque and utilize the presented guidelines for the choice of the air gap radius.

TABLE I
Simulation Parameters (equal for both setups)

Parameter	Symbol	Simulation values
No. of stator teeth		4
Pole pair number	p	6
Machine radius	R	100 mm
Machine length	l	20 mm
Air gap radius	r	10…92.5 mm
Magnet thickness	δ_{PM}	5 mm
Air gap thickness	δ	0.5 mm
Winding space factor	c_w	0.1…0.9
Tooth width	w_t	$\sqrt{2}\cdot(1-\sqrt{c_w})\cdot r$
Current density	J	5 A/mm^2
Copper fill factor	k_{cu}	0.5
Iron material (real)	M270–35A	$B_{sat} \approx 1.6$ T
Iron material (ideal)		$\mu_r = 6000$; $B_{sat} \rightarrow \infty$
Magnet material	NdFeB	$B_r = 1.2$ T

References

[1] A. Parviainen, M. Niemela, J. Pyrhonen, J. Mantere, "Performance comparison between low-speed axial-flux and radial-flux permanent-magnet machines including mechanical constraints," *IEEE IEMDC,* pp. 1695-1702, May 2005.

[2] M. Kitamura, J. Kaneda, N. Hino, "Motor design approach utilizing regularity of a two-dimensional magnetic field," *IEEE Trans. Mag.,* vol. 39, no. 3, pp. 1464-1467, May 2003.

[3] S. Huang, J. Luo, F. Leonardi, and T. A. Lipo, "A general approach to sizing and power density equations for comparison of electrical machines," *IEEE Trans. on Industry Applications*, IA-34, no. 1, pp. 92-97, 1998.

[4] S. Wu, L. Song, S. Cui, "Study on Improving the Performance of Permanent Magnet Wheel Motor for the Electric Vehicle Application," *IEEE Trans. Mag.*, vol. 43, no. 1, pp. 438-442, Jan. 2007.

[5] L. Hsu, M. Tsai, C. Huang, "Efficiency optimization of brushless permanent magnet motors using penalty genetic algorithms," *IEEE IEMDC*, vol. 1, pp. 365-369, June 2003.

[6] C. Espanet, A. Miraoui, J.-M. Kauffmann, "Optimal design of an high torque DC brushless in-wheel motor," *IEEE IEMDC,* vol. 3, pp. 1402-1409, June 2003.

[7] J. R. Hull and L. R. Turner, "Magnetomechanics of internal-dipole Halbach-array motor/generators," *IEEE Trans Mag.,* vol. 36, pp. 2004-2011, 2000.

[8] M. Rizzo, A. Savini, and J. Turowski, "Influence of number of poles on the torque of DC brushless motors with auxiliary salient poles," *IEEE Trans. Mag.*, vol. 27, pp. 5420-5422, Nov. 1991.

[9] V. B. Honsinger, "Sizing equations for electrical machinery," *IEEE Trans. Energy Convers.*, vol. 2, no. 1, pp. 116-121, Mar. 1987.

[10] Maxwell 3D by Ansoft Corporation [Online]. Available: http://www.ansoft.com.

Manuscript received March 6, 2009. Corresponding author: T. Reichert (e-mail: reichert@lem.ee.ethz.ch; +41 44 633 77 91).